An analytical study of the impact of glazed vs diffuse facades on solar trapping with detailed directional radiation model

Delia Valledor, Georgios Kyriakodis, Anne Penillard, Emmanuel Bozonnet

6th International Conference on Building Energy and Environment
Eindhoven University of Technology, The Netherlands
6 - 10 July 2025

An analytical study of the impact of glazed vs diffuse facades on solar trapping with detailed directional radiation model

Delia Valledor[1,2,3], Georgios Kyriakodis[2], Anne Penillard[1], Emmanuel Bozonnet[3]

[1] *Saint-Gobain Recherche, Paris, France, delia.valledor@saint-gobain.com*
[2] *CSTB, Sophia-Antipolis, France, georgios.kyriakodis@cstb.fr*
[3] *LaSIE UMR CNRS 7356, La Rochelle, France, emmanuel.bozonnet@univ-lr.fr*

SUMMARY

The optical properties of building envelopes govern the inward and outward energy fluxes of a city; and therefore play a major role in urban overheating due to solar trapping. High reflectance (cool) materials have demonstrated a reduction in surface temperature of roofs with a high sky view factor, but their effects are limited to the upper floors of the buildings. To address the root cause of solar trapping, we must focus our attention on facades and roads, as these are the surfaces that contribute to multireflections in densely populated areas. We will showcase the interrelation between the shortwave optical properties of facades and the leading reflections within the canyon.

We have developed an analytical urban canyon model that integrates a detailed angular shortwave radiation description of materials. We aim to quantify the impact of the optical properties of building facades on solar trapping by analyzing the directionality of their reflections. We track the irradiance reflected toward the road and toward the buildings, as they will affect pedestrian thermal comfort and building cooling needs, respectively. We consider traditional materials (lambertian and specular) to evaluate the current situation, and innovative materials (retroreflective) to envision solar trapping mitigation strategies. Simulations are performed with an hourly time step for a year time period.

To verify the consistency of the model, we present the results for a mediterranean compact midrise neighborhood (H/W=1). During summer, for East-West facade orientations, glazed facades contribute to a 15 % increase of ground peak irradiance (equivalent to 85 W/m^2) compared to typical lambertian facades. The contribution of solar irradiance to thermal stress is evaluated with temperature sol-air indicator. Specular canyons result in a rise of 2°C in peak sol-air temperature. For a typical meteorological year, specular facades increase by 11 % (155) the sol-air degree-hours above 26°C, and increase by 132 % (145) the degree-hours above 40°C compared to lambertian facades. Future studies will focus on measuring the impact on thermal comfort and building energy performance at neighborhood scale.

Keywords: urban canyon model, urban radiative model, solar trapping.

1. INTRODUCTION

Urban overheating is a major problem in densely populated areas, leading to the degradation of thermal comfort and and increase in health problems (Santamouris, 2020). This positive energy balance is primarily driven by a radiative solar trapping phenomenon, resulting from a combination of multiple factors: (1) narrow and deep canyons, which facilitate shortwave multireflections and limit longwave cooling exchanges with the sky, and (2) high-capacity materials that store energy during the day and release it at night. Anthropogenic heat release (urban traffic and other contributions such as air conditioners), and the scarcity of green areas contribute to urban overheating.

High reflectance (cool) materials have proven to be an effective mitigation strategy to cool down surfaces with a high sky view factor (roofs). However, when applied to other urban surfaces (i.e. vertical facades), they increase the multireflections, what consequently penalize neighboring buildings and pedestrian comfort. In recent years, researchers have started to focus their attention toward retroreflective materials. These materials are engineered in such a way that they reflect the incoming shortwave radiation back toward the source and limit the multireflections with surrounding surfaces, hence solar trapping. Retroreflective materials have shown promising results when applied to urban facades both experimentally (Rossi et al., 2015) and numerically (Kyriakodis, Schiavoni, et al., 2023). They have proven to lower ground surface temperature, to improve in pedestrian thermal comfort and to reduce energy consumption.

This article aims to isolate shortwave radiation from other heat transfer mechanisms in order to build a fundamental understanding of how the shortwave directional properties of urban materials—lambertian, specular, and retroreflective—impact irradiance within an urban canyon. To achieve this, we have developed an analytical bidimensional urban canyon model.

2. METHODOLOGY

This section describes an bidimensional urban canyon model that we have developed.

2.1. Shortwave radiation model

This model describes the dynamics of shortwave radiation in an urban canyon. The total solar irradiance on a surface (E) is the result of the combination of the direct (beam) irradiance (E_b), the diffuse irradiance (E_d), as well as the multireflections between the surfaces (E^*), as described in Equation 1 (Duffie and Beckman, 2013).

$$E = E_\mathrm{b} + E_\mathrm{d} + E^* \tag{1}$$

Surface material properties are defined by their angular reflectance $\rho^\mathrm{mat}(\theta)$, which allows to compute the angular reflected irradiance of a material by considering the instantaneous beam irradiance. The novelty of this model is the explicit calculation of the first beam reflection $E_\mathrm{rb}^\mathrm{mat}$ as a function of the angular reflectance of the material (Equation 2). This allows to track the amount and the direction of this reflected radiation (material models explained in 2.1.3). The following reflections are computed following the radiosity model (Gros et al., 2011).

$$E_\mathrm{rb}^\mathrm{mat}(\theta) = \rho^\mathrm{mat}(\theta) \times E_\mathrm{b} \tag{2}$$

The sun position is defined by the solar elevation angle h_{sun} and the solar azimuth ϕ_{sun}. The urban canyon geometry is defined by the building height (H) and the street width (W). Each urban

surface is characterized by the tilt angle χ_{surf} measured with respect to the horizontal plane and an azimuth angle ϕ_{surf} defined clockwise with respect to the North. Solar masks link solar position with surface position, indicating for a given surface whether the surface is being irradiated or not for every time step. As observed in Equation 3, solar masks are defined as boolean Ψ_{surf} that are true if the surface is irradiated.

$$\Psi_{\text{surf}} = \sin h_{\text{sun}} \times (\cos(\phi_{\text{sun}} - \phi_{\text{surf}}) \times \sin \chi_{\text{surf}} + (h_{\text{sun}} > \arctan(H/W)) \times \cos \chi_{\text{surf}}) > 0 \tag{3}$$

For an irradiated surface, the total angle of incidence of the solar irradiance θ_{i} is computed with Equation 4. The angle of incidence is 0° if normal to the surface, and 90° if tangent.

$$\cos \theta_{\text{i}} = \cos h_{\text{sun}} * \cos(\phi_{\text{sun}} - \phi_{\text{surf}}) * \sin \chi_{\text{surf}} + \sin h_{\text{sun}} * \cos \chi_{\text{surf}} \tag{4}$$

The irradiated surface per meter depth of canyon of a vertical building facade ($x_{\text{s}}^{\text{bld}}$) and the street pavement ($x_{\text{s}}^{\text{pav}}$) are computed as a function of solar elevation and the canyon dimensions with Equations 5 and 6 respectively.

$$x_{\text{s}}^{\text{bld}} = \min(|W * \tan h_{\text{sun}}|, H) \tag{5}$$

$$x_{\text{s}}^{\text{pav}} = W - \min\left(\left|\frac{H}{\tan h_{\text{sun}}}\right|, W\right) \tag{6}$$

2.1.1. Reflection of building facades

When considering a vertical building facade, one can compute the total reflected irradiance in W/m (per meter of depth) toward the street and the building, as shown in Equations 7 and 8.

$$x_{\text{s}}^{\text{bld}}(t) * E_{\text{rb}}^{\text{bld}\to\text{pav}}(t) = \int_0^{x_{\text{s}}} \int_{-90}^{\theta_{\text{pav-bld}}} E_{\text{rb}}(\theta, t)\, d\theta\, dx \tag{7}$$

$$x_{\text{s}}^{\text{bld}}(t) * E_{\text{rb}}^{\text{bld}\to\text{bld}}(t) = \int_0^{x_{\text{s}}} \int_{\theta_{\text{pav-bld}}}^{\theta_{\text{bld-sky}}} E_{\text{rb}}(\theta, t)\, d\theta\, dx \tag{8}$$

Where the integration limits can be calculated with Equations 9 and 10. Note that the integration limits are computed at x, that stands for each of the 10 discretized elements of x_{s}.

$$\theta_{\text{pav-bld}}^{\text{bld}} = -90 + \arctan\frac{W}{H - x} \tag{9}$$

$$\theta_{\text{bld-sky}}^{\text{bld}} = 90 - \arctan\frac{W}{x} \tag{10}$$

2.1.2. Reflection on pavement

Similarly, when considering a horizontal pavement, one can compute the total reflected irradiance in W/m (per meter of depth) toward the building on the right with Equation 11.

$$x_s(t) * E_{rb}^{\text{pav}\rightarrow\text{bld right}}(t) = \int_0^{x_s} \int_{-90}^{\theta_{\text{bld right}}} E_{rb}(\theta, t)\, d\theta\, dx \tag{11}$$

Equation 12 computes the integration limit of the equation above. Note that the integration limit is computed at x, that stands for each of the 10 discretized elements of x_s.

$$\theta_{\text{bld right-sky}}^{\text{pav}} = \begin{cases} -90 + \arctan\frac{H}{W-x}, & \text{if } \cos(\phi_{\text{sun}} - \phi_{\text{bld left}}) \geq 0 \\ 90 - \arctan\frac{H}{x}, & \text{otherwise} \end{cases} \tag{12}$$

2.1.3. Material models for first direct (beam) reflection

The definition the angular reflection material models is the key of this model. The three material models used in this study can be visualized in Figure 1: lambertian, specular and retroreflective.

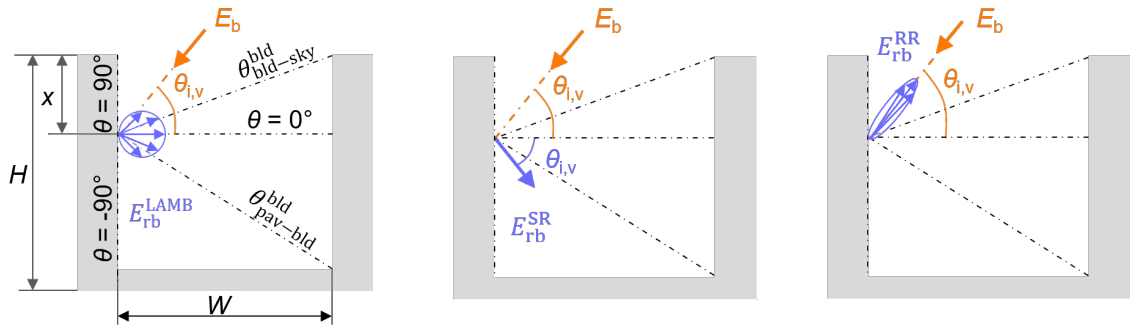

(a) Lambertian (LAMB) **(b)** Specular Reflective (SR) **(c)** Diffuse Retroreflective (RR)

Figure 1. Schematic of the beam first reflection for urban canyons with (a) lambertian, (b) specular and (c) retroreflective facades.

Lambertian (LAMB, Figure 1a) model represents matte or rough diffuse surfaces such as concrete or paintings. The reflected irradiance directs toward every point in the space, as described by Equation 13.

$$E_{rb}^{LAMB} = E_b \int \rho^{LAMB} \cos\theta\, d\theta \tag{13}$$

Specular Reflective (SR, Figure 1b) model represents very smooth materials such as glazing. The reflected irradiance presents a form of a point ray in a direction that is symmetrical to the angle of incidence with respect to the facade, as described by Equation 14.

$$E_{rb}^{SR} = E_b \int \rho^{SR} \delta(\theta - \theta_i)\, d\theta \tag{14}$$

Diffuse Retroreflective (RR, Figure 1c) model represents innovative materials that reflect radiation mostly in the direction of incidence. The reflection follow a Lafortune lobe (with concentration factor $n = 15$), as described by Equation 15.

$$E_{rb}^{RR} = E_b \int \rho^{RR} \cos(\theta - \theta_i)^n\, d\theta \tag{15}$$

2.2. Metric for thermal stress

Temperature sol-air ($T_{\text{sol-air}}$) is the chosen indicator to measure the contribution of irradiance to thermal stress. This is a standard equivalent temperature that includes both convective and radiative heat transfer to calculate the temperature of the considered surface using the overall irradiance. It is calculated with Equation 16:

$$T_{\text{sol-air}} = T_{\text{amb}} + \frac{\alpha \times E}{h_{\text{e}}} \tag{16}$$

Where T_{amb} stands for the air temperature from the weather file, α is the material shortwave absorptivity and h_{e} is the equivalent (convective and radiative) heat transfer coefficient. According to the Standard EN ISO 6945 h_{e} is set to 25 W/Km^2.

2.3. Case study

This study analyzes an infinite urban canyon along the axis North-South located in a compact midrise neighborhood (H/W=1) with mediterranean climate (Nice, South of France) for a typical meteorological year. We aim to evaluate the impact of the optical properties of the urban surfaces (facades) on the solar irradiance distribution within the canyon and the pedestrian thermal stress. More specifically, we will compare lambertian reflection representing residential buildings with low window-to-wall ratio; specular reflection, representing glazed facade buildings of financial districts; and retroreflection, representing innovative facades with diffuse retroreflective properties.

To compare these three reflective properties in realistic conditions, typical material properties have been chosen according to Saint-Gobain database. lambertian facades are defined with 30 % albedo. Specular facades present an angular dependent albedo varying between 40 and 90 %, with average value of 50 % and an average absorption of 26 %. Retroreflective materials present an albedo of 60 %. The street presents an albedo of 15 % (Kyriakodis and Santamouris, 2018).

3. RESULTS

This section presents the results of irradiance and temperature sol-air for a North-South urban canyon (H/W=1) with a mediterranean climate.

3.1. Daily solar irradiance

June 23 has been selected as a representative day in summer, the closest to the summer equinox with high sky clearance. Figure 2 shows the total solar irradiance on a West facade and the ground analyzed on an hourly basis for the three materials examined in this study. Irradiance values are normalized by the area of the respective surfaces. Yellow shaded areas represent the solar direct and diffuse irradiance; dark and light pink shaded areas stand for the reflected radiation from the East and West facades respectively; green shaded areas represent the reflected radiation from the ground; and gray areas represents multireflections.

We can observe that the direct and diffuse irradiance components are consistent across all West facades and the ground. Peak irradiance occurs at 17:00 for the West facade and at 13:00 for the ground. The daily direct and diffuse radiant exposure amounts to 1800 Wh/m^2 for the West facade and 2900 Wh/m^2 for the ground.

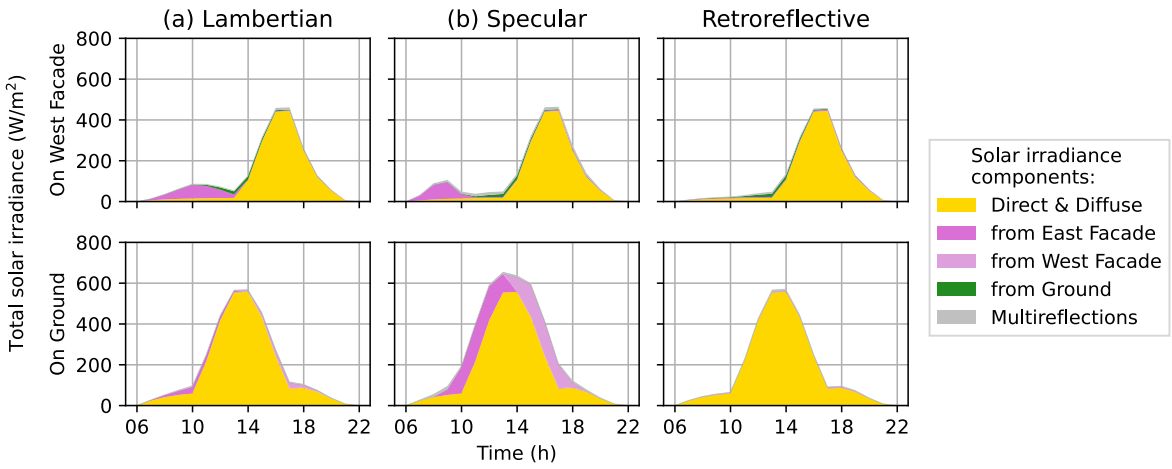

Figure 2. Total shortwave irradiance on West facade (first row) and ground (second row) on June 23 for a H/W=1 urban canyon with (a) lambertian, (b) specular and (c) retroreflective facades.

West facades in both lambertian and specular canyons experience a 230 Wh/m^2 (10 %) increase in radiant exposure compared to retroreflective canyons, primarily due to reflections from the east-facing facades. Specular East facades reflect solar irradiance toward the West facade in the early morning (before 10h), while lambertian east facades reflect irradiance until 13h. Peak irradiance remains equal for the three canyons. The contribution from the ground represents 3 % of the total daily irradiance.

The radiant exposure on the ground of a specular canyon is 970 Wh/m^2 higher than lambertian canyon and 1140 Wh/m^2 higher than a retroreflective canyon. Specular reflection by the East facade increases by 40 % the total daily irradiance on the ground compared to retroreflective canyons. Peak irradiance increases by 85 W/m^2 (15 %) due to specular reflection compared to canyons with lambertian and retroreflective facades.

3.2. Annual solar irradiance on facades

The total solar irradiance on the West facade for a typical meteorological year is presented in Figure 3 in terms of W/m^2 for every hour of the year for a H/W=1 urban canyon with lambertian, specular and retroreflective facades. Total irradiance includes direct, diffuse and reflections from the surrounding surfaces (East facade and Ground). White areas indicate no irradiance, dark intensity indicates higher irradiance.

We can observe that all lambertian, specular and retroreflective facades are irradiated between 13h and 20h, this corresponds to direct and diffuse irradiance, and reflection from the ground. Unlike retroreflective facades, that are only irradiated during these period, lambertian and specular facades are also irradiated between 6h and 13h due to reflections from the East facade. Specular facades present a thinner irradiated region during the morning period. Annual peak irradiance is up to 589 W/m^2 in both lambertian and specular canyons, 1.5 % higher than retroreflective facades. Regarding the daily radiant exposure for the year period, specular canyons increase the annual peak by 9 % compared to retroreflective canyons.

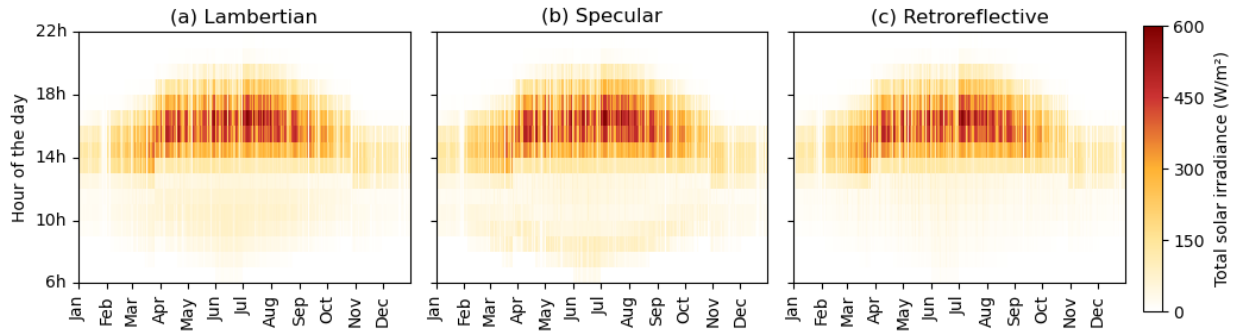

Figure 3. Total shortwave irradiance on West facade (direct, diffuse and reflections) for a H/W=1 urban canyon with (a) lambertian, (b) specular and (c) retroreflective facades.

3.3. Irradiance contribution to thermal stress

The temperature sol-air for the ground for a typical meteorological year is presented in Figure 4 for every hour of the year for canyons with lambertian, specular and retroreflective facades.

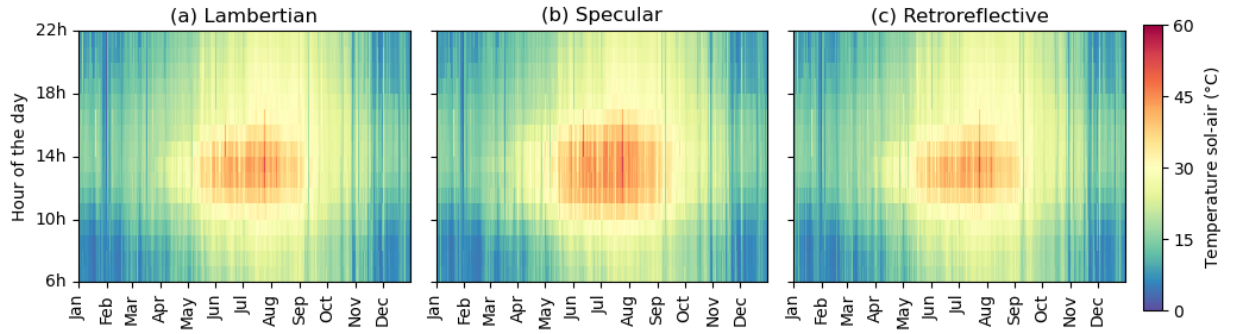

Figure 4. Temperature sol-air on ground for a H/W=1 urban canyon with (a) lambertian, (b) specular and (c) retroreflective facades.

Specular canyons lead to a maximum annual temperature sol-air of 54°C, that is 2°C higher than lambertian and retroreflective canyons. Specular canyons lead to 1555 degree-hours/year of temperature sol-air above 26°C, that is 155 degree-hours (11 %) more than lambertian canyons and 210 degree-hours (16 %) more than retroreflective canyons. Sol-air temperatures above 26°C occur between April and October.

Specular canyons result in 255 degree-hours per year of sol-air temperatures exceeding 40°C, which is 145 degree-hours (132 %) higher than lambertian canyons and 150 degree-hours (143 %) higher than retroreflective canyons. These sol-air temperatures above 40°C are observed between May and August.

4. CONCLUSIONS AND PERSPECTIVES

This study aims to improve our understanding of shortwave irradiance and interreflections between surfaces by examining typical materials—Lambertian, specular, and retroreflective. To achieve this, we developed a bidimensional urban canyon model that accounts for the angular reflectance of these materials. Our findings demonstrate consistent differences between the three models, emphasizing the need for caution when using radiosity algorithms to model all surfaces within a neighborhood, especially in the presence of large specular surfaces.

For an urban canyon with a height-to-width ratio of $H/W = 1$ in a Mediterranean climate (Nice, South of France), specular facades (with angular-dependent albedo ranging from 40 % to 90 %) result in a 15 % increase in peak irradiance on the ground (85 W/m^2) compared to lambertian (30 % albedo) and retroreflective (60 % albedo) canyons. This increase in peak irradiance contributes to a higher thermal stress, measured using the sol-air temperature indicator. Specifically, specular canyons lead to an increase of 225 degree-hours per year (+143 %) above 40°C compared to lambertian canyons. This study highlights the strong correlation between shortwave radiation directionality and thermal stress.

Beyond this first approach to demonstrate the issues of specular materials in dense cities and the potential of innovative retroreflective materials, we will exploit this fast analytical model (1 minute calculation time for an annual analysis) to perform an extensive parametric analysis on aspect ratio, street orientation and geolocation for different materials. Besides we are conducting an experimental validation and intermodel comparisons that will be published soon. Then, we will develop a three-dimensional multiphysics model to asses neighborhood configurations and quantify the impact of urban surfaces on thermal comfort and building energy performance, building upon the promising results presented by Kyriakodis, Schiavoni, et al. (2023).

ACKNOWLEDGMENTS

The authors would like to thank the ANRT for supporting the contract CIFRE 2023/1818.

REFERENCES

Duffie J. A. and Beckman W. A., 2013. Solar Engineering of Thermal Processes. John Wiley & Sons, Ltd.

Gros A., Bozonnet E., and Inard C., May 2011. Modelling the Radiative Exchanges in Urban Areas: A Review. Advances in Building Energy Research 5, 163–206.

Kyriakodis G.-E., Schiavoni M., Riederer P., Bozonnet E., Anne P., and Xavier C., Dec. 2023. Impact of retro-reflective windowpanes on building energy demand and pedestrian thermal comfort under various neighborhood settlements. Proceedings of 6th International Conference on Countermeasures to Urban Heat Islands (IC2UHI). Ed. by P. Rajagopalan, V. Soebarto, and H. Akbari. RMIT University. Melbourne (AUS), Australia, 1097–1106.

Kyriakodis G.-E. and Santamouris M., June 2018. Using Reflective Pavements to Mitigate Urban Heat Island in Warm Climates - Results from a Large Scale Urban Mitigation Project. Urban Climate 24, 326–339.

Rossi F., Morini E., Castellani B., Nicolini A., Bonamente E., Anderini E., and Cotana F., Oct. 2015. Beneficial Effects of Retroreflective Materials in Urban Canyons: Results from Seasonal Monitoring Campaign. Journal of Physics: Conference Series 655, 012012.

Santamouris M., Jan. 2020. Recent Progress on Urban Overheating and Heat Island Research. Integrated Assessment of the Energy, Environmental, Vulnerability and Health Impact. Synergies with the Global Climate Change. Energy and Buildings 207, 109482.